

CHAPTER 3

MOLECULAR DETERMINANTS OF TRPC6 CHANNEL RECOGNITION BY FKBP12

PENG TAO,¹ JOHN C. HACKETT,² JU YOUNG KIM,³
DAVID SAFFEN,⁴ CARRIGAN J. HAYES,⁵
and CHRISTOPHER M. HADAD⁶

¹*Department of Chemistry, Southern Methodist University,
3215 Daniel Avenue, Dallas, Texas 75275-0314, USA,
E-mail: ptao@smu.edu*

²*Institute for Structural Biology and Drug Discovery, Virginia
Commonwealth University, 800 East Leigh Street, Richmond,
Virginia 23219, USA*

³*Institute for Cell Engineering, Johns Hopkins University School
of Medicine, 733 N Broadway, Baltimore, Maryland 21205, USA*

⁴*Department of Cellular and Genetic Medicine, School of Basic
Medical Sciences, Fudan University, 130 Dongan Rd, Shanghai
200032, P.R. China*

⁵*Department of Chemistry, Otterbein University,
1 South Grove Street, Westerville, Ohio 43081, USA*

⁶*Department of Chemistry, The Ohio State University,
100 W. 18th Ave., Columbus, Ohio 43210, USA*

CONTENTS

Abstract.....	70
3.1 Introduction.....	71
3.2 Computational Methods.....	73
3.3 Results and Discussion.....	78
3.4 Conclusions.....	92
Acknowledgments.....	93
Keywords.....	93
References.....	94

ABSTRACT

Transient receptor potential-canonical 6 (TRPC6) calcium channels are currently the subject of intense investigation due to their roles in modulating smooth muscle tone in blood vessels and lung airways. TRPC6 channels are also proposed to mediate physiological processes in the kidney, immune system and central nervous system. We previously reported that binding of the immunophilin FKBP12 (FK506 binding protein–12 kDa) to a TRPC6 intracellular domain is a prerequisite for the formation of a multi-protein complex involved in channel regulation. This study also demonstrated that binding of FKBP12 to TRPC6 requires prior phosphorylation of Ser768 in the putative TRPC6 binding domain. To study the elements of molecular recognition in FKBP12 for the TRPC6 intracellular domain, we performed molecular dynamics simulations in explicit solvent on model complexes containing FKBP12 and the following: (i) the unphosphorylated wild-type TRPC6 intracellular binding domain, (ii) the wild-type TRPC6 binding domain containing a phosphorylated Ser768 residue, and (iii) TPRC6 peptides in which Ser768 was replaced with Asp or Glu. Simulations using the Generalized Born/Surface Area model (MM-GB/SA) predicted favorable binding and small conformational fluctuations for the FKBP12/phosphorylation Ser768 TRPC6 peptide complex, due to the strong interactions between the phosphate group and Lys44, and Lys47 residues in the FKBP12 binding site. Decomposition of the binding free energies into each amino acid residue identified additional important structural elements necessary for this protein-protein interaction.

3.1 INTRODUCTION

Transient receptor potential-canonical (TRPC) channels are members of the mammalian TRP channel superfamily of cation channels [1, 2]. The seven known subtypes of TRPC channels (TRPC1–7) are widely expressed in cells and tissues, where they mediate the influx of extracellular Ca^{2+} and/or Na^{+} in response to the activation of cell surface receptors. These influxes regulate key cellular functions, including contraction of smooth muscle, activation of immune cells, mobility of neuronal growth cones, and cell proliferation and migration. Because many of these functions are relevant to human disease, there is currently considerable interest in developing agents that activate or inhibit TRPC channels for use as therapeutic drugs [3–6].

Native TRPC channels comprise four protein subunits, which are symmetrically organized around a central pore. Each subunit contains six transmembrane (TM) domains and a single membrane-loop domain (located between TM5 and TM6) that contributes to the channel pore. The amino- and carboxyl-termini of each subunit are located on the intracellular side of the membrane. TRPC3, TRPC6 and TRPC7 channels are structurally and functionally related and constitute a subfamily of TRPC channels [7, 8]. Each of these subtypes can form homotetrameric channels or combine with other subfamily members to form heterotetrameric channels.

Understanding the molecular mechanisms involved in the regulation of TRPC channels will be important for the identification of novel drug targets for TRPC channel-regulated processes. Moreover, these have motivated the search for post-translational modifications that alter the function of TRP channels [9] and proteins that interact with the channels [10]. As mentioned above, TRPC3/6/7 channels are regulated by PKC, which phosphorylates the channels on a conserved serine residue in the carboxyl-terminal region (Ser712 in TRPC3 [11] and Ser714/Ser768 in TRPC6A/B [12]). By contrast, phosphorylation of TRPC3 by Src [13] and TRPC6 src-family tyrosine kinases [14] is required for maximal channel activation. TRPC3/6/7 channels have also been shown to directly bind several proteins including the calcium binding protein calmodulin [15, 16], the IP3 receptor of the endoplasmic reticulum [17] and the adapter protein Homer [18, 19]. Studies by Schiling et al. [20] have shown that TRPC3/6/7 channels also contain a binding site for the immunophilin FKBP12 (FK506 binding protein–12 kDa)

within the carboxyl-terminal cytoplasmic domain. Site-specific mutagenesis studies demonstrated that FKBP12 binds to the consensus sequence LPXPFYLVPSPK ($X = P, V$ or S ; $Y = S$ or N). The serine residue within this segment is the target for PKC phosphorylation: Ser768 in the TRPC6A splice variant and Ser714 in the TRPC6B splice variant.

We previously showed that FKBP12 is a component of a TRPC6-centered protein complex that rapidly forms following activation of endogenous M_1 mAChR [12]. Data from that study suggest that the following events take place following activation of M_1 mAChR with carbachol. First, a protein complex containing M_1 mAChRs, TRPC6 channels and PKC rapidly assembles within the cell membrane. Second, PKC phosphorylates the TRPC6 channels on Ser768/Ser714. Third, phosphorylation of Ser768/Ser714 creates a binding site for FKBP12. Fourth, binding of the FKBP12 to TRPC6 results in the recruitment of the calcineurin/calmodulin to the complex. Finally, the channels are dephosphorylated by the calcineurin, releasing M_1 mAChR from the complex.

A novel aspect of the above sequence of events is the observation that TRPC6 channel phosphorylation by PKC is required for the binding of FKBP12. Evidence for this includes the observation that coimmunoprecipitation of the channels and FKBP12 is blocked when channel phosphorylation is attenuated by PKC inhibition or by substitution of Ser768/Ser714 with alanine or glycine [12]. Taken together, these studies show that phosphorylation of TRPC6 channels by PKC and the subsequent binding of FKBP12 play a central role in the regulation of TRPC6 channel trafficking and, thus, indirectly regulate TRPC6 channel activity. As described below, these studies implicate specific amino acid residues within each protein and predict that binding requires phosphorylation of Ser768/Ser714.

Molecular dynamics (MD) simulations and binding free energy calculations using implicit solvent models are powerful tools to study the interactions between biomacromolecules. It has been shown in numerous studies that simulation of protein-ligand complexes can provide detailed insight into ligand binding modes. Furthermore, their binding free energies may be accurately using a combination of molecular mechanics internal energies, solvation free energies, and vibrational entropies [21–29]. Recently, the Generalized born (GB) method was improved to produce comparable results with Poisson–Boltzmann (PB) method with much reduced computational cost [30, 31].

All of these computational advantages make calculation of binding free energy of protein complexes based on MD trajectory feasible. In particular, there is significant precedent for application of these computational methods for calculation of ligand binding free energies to FKBP12 [32–36]. In this chapter, these techniques are successfully applied to expand our understanding of the determinants of the FKBP12-TRPC6 protein-protein interaction.

3.2 COMPUTATIONAL METHODS

3.2.1 TRPC6 PEPTIDE DOCKING

A prerequisite for using MD to study protein-peptide interactions is a template that provides information about the location and nature of the peptide binding site on the receptor protein. To date, co-crystal structures of FKBP12 have been determined with fragments of the TGF- β receptor Type I (TGF β TRI; PDB entry: 1B6C) [37], bone morphogenetic protein receptor type-1B (PDB entry: 3MDY) [38], and the kinase domain of the type I activin receptor (PDB entry: 3H9R) [39]. In each structure, FKBP12 predominantly interacts with a leucyl-prolyl-initiated α -helix on the C-terminal side of the binding partner GS domain. The structure of FKBP12, partner α -helix, and binding mode are essentially identical in the three protein complexes. Furthermore, the amino acid sequences of the leucyl-prolyl-initiated peptides constituting these α -helices are also strongly conserved. The strong sequence and structural conservation in these protein-protein interactions are illustrated in the Figure 1. Sinkins and co-workers demonstrated that the analogous leucyl-prolyl-initiated peptide ⁷⁵⁹LPVVPFNLVPSP⁷⁶⁹ of TRPC6 mediates its interaction with FKBP12 [20]. Since this sequence has been demonstrated experimentally to mediate the FKBP12-TRPC6 interaction and the structure of FKBP12 domains of similar sequences are strongly conserved, the structure of the TRPC6 peptide was initially modeled on the α -helical structure of the TGF β TRI peptide.

To generate the initial geometries of the TRPC6 peptide, the ¹⁹³LPLLVQRTIAR²⁰³ helix was excised from the crystal structure of the FKBP12-TGF- β receptor Type I fragment complex, and the amino acids corresponding to those found in TRPC6 were introduced. In addition to

the unphosphorylated and phosphorylated wild-type peptides, Ser768Asp and Ser768Glu mutants were also modeled. Each peptide was capped with methyl and acetyl groups at the N- and C-terminal ends, respectively. These peptides were then fully optimized using the AMBER ff94 force field [40]. Possible modes of peptide binding were explored using the DOCK 5.2.0 suite of programs [41], to generate initial structures for MD simulations. In doing so, the FKBP12 receptor was extracted from PDB structure 1B6C; protons were added in a manner consistent with physiological pH; and charges from the ff94 force field were applied. In docking calculations, the helical peptides were oriented into the FKBP12 binding site as a rigid body considering a maximum of 2×10^6 orientations. Torsional angles in the peptides for each binding mode were minimized to optimize the total energy score using the simplex minimizer in the DOCK suite of programs [42, 43]. Additional details of the docking methodology and energy scores for the peptides are listed in Table 3.1.

3.2.2 MD SIMULATION OF FKBP12-TRPC6 PEPTIDE COMPLEXES AND ISOLATED BINDING PARTNERS

In addition to the four FKBP12-TRPC6 peptide complexes, MD simulations of the isolated species (FKBP12 and the various TRPC6 peptides)

TABLE 3.1 DOCK Energy Scores (kcal/mol) for the Preferred Modes of TGF- β Receptor Type I and TRPC6 Peptides Binding to the FKBP12 Receptor^a

Peptide	Van der Waals	Electrostatic	Total Energy Score
LPLLVQRTIAR ^b	-36.2	-1.4	-37.6
LPVVPFNLVSP	-36.3	-3.5	-39.8
LPVVPFNLVPPSP	-28.4	-12.3	-40.7
LPVVPFNLVDP	-33.6	-5.0	-38.5
LPVVPFNLVPEP	-31.1	-12.5	-43.6

^aA Connolly solvent-accessible surface of FKBP12 was generated with a probe radius of 1.4 Å for input to the SPHGEN program, from which a set of 57 overlapping spheres defining the FKBP12 binding pocket was created. DOCK scoring grids with dimensions of 42×34×24 Å were created with the GRID program, using electrostatic potential charges from ff94 and van der Waals parameters from the ff99 force field.

^bTGF- β receptor Type I peptide.

were also conducted. For FKBP12 alone, the initial structure was taken from the crystal structure (PDB ID: 1B6C), and the initial structures of the four peptides were prepared as noted above. All of the MD simulations were conducted with the AMBER 8 suite of programs [44]. The all-atom force field ff03 of Duan et al. [45] was used, and the simulations were conducted with explicit water solvent, represented by the TIP3P model [46]. Proteins and protein-peptide complexes were immersed in a box of water, with a minimum distance of 10 Å between the protein complex and the box surface, and included approximately 20,000 atoms. Periodic boundary conditions were applied, using the particle mesh Ewald [47–51] method for the long-range electrostatic treatment. The SHAKE bond-length constraint method [52] was applied to constrain the length of covalent bonds containing hydrogen during the simulations. A non-bonded interaction cutoff value of 8 Å was used. After initial optimization, all of the systems were equilibrated in 4000 steps, and heated from 0 to 300 K in the NVT ensemble. Then, 20 ns production runs were conducted under isothermal-isobaric ensemble (NPT) conditions, at 300 K and 1 bar. A time constant of 1.2 ps was used for heat bath coupling, and 2.0 ps was used as the relaxation time for pressure regulation [53]. The time step was 1 fs for all of the 20 ns MD simulations, and in each case, coordinates were saved every 100 steps. Details of each simulation system are listed in Table 3.2.

TABLE 3.2 MD Simulation Details of FKBP12, Probe Peptides and Their Complexes

Structure	Water Molecule Number	Box Dimension (Å)	Length of the simulation (ns)	Equilibrium Time (ps)
FKBP12	5603	58×72×58	20	4
WT	3502	55×51×50	20	4
pWT	3526	54×55×49	20	4
Ser768Asp	3423	50×57×50	20	4
Ser768Glu	3442	50×56×50	20	4
FKBP12-WT	5525	58×72×58	20	4
FKBP12-pWT	5681	58×72×60	20	4
FKBP12-Ser768Asp	5614	58×72×59	20	4
FKBP12-Ser768Glu	5643	58×72×59	20	4

3.2.3 MM/GB-SA FREE ENERGY OF BINDING CALCULATIONS

For each peptide, the free energy of binding to FKBP12 was computed using the MM-GB/SA method [54], available in the AMBER program suite. This method uses a thermodynamic cycle to calculate the free energy of binding for each ligand, in this case the TRPC6-derived peptides, to the FKBP12 receptor [55, 56]. The free energies of binding are computed using the equation:

$$\Delta G_{binding}^{sol} = \Delta G_{complex}^{sol} - \Delta G_{receptor}^{sol} - \Delta G_{ligand}^{sol} \quad (1)$$

where $\Delta G_{binding}^{sol}$ is the total free energy of binding in solution, and $\Delta G_{complex}^{sol}$, $\Delta G_{receptor}^{sol}$ and ΔG_{ligand}^{sol} are free energies in solution of the complex, receptor and ligand, respectively. The free energy in solution of each entity (ΔG^{sol}) is calculated by the following equations:

$$\Delta G^{sol} = \Delta G^{gas} + \Delta G_{solvation} \quad (2)$$

$$\Delta G^{gas} = E_{internal} + E_{vdw} + E_{electrostatic} - T\Delta S \quad (3)$$

$$\Delta G_{solvation} = \Delta G_{GB} + \Delta G_{nonpolar} \quad (4)$$

where ΔG^{gas} is the free energy in gas phase, and $\Delta G_{solvation}$ is the solvation energy. ΔG^{gas} is the sum of the internal energy ($E_{internal}$), van der Waals (E_{vdw}) and Coulombic ($E_{electrostatic}$) interaction, as well as entropic contributions (ΔS). The internal energy includes bond stretching, bond angle, and torsional contributions to the total molecular mechanics (MM) energies. The solvation energy $\Delta G_{solvation}$ includes polar (ΔG_{GB}) and non-polar contributions ($\Delta G_{nonpolar}$). The thermodynamic cycle for binding free energy calculation is illustrated in Figure 3.1.

For a given FKBP12 TRPC6 peptide complex, the MM-GB/SA method requires snapshots from the MD trajectories for that complex, as well as from those of FKBP12 and the peptide alone. The first 2 ns of the MD simulation were considered as an equilibration period and were discarded for the free energy of binding calculations. For each complex, 1,000 snapshots were evenly extracted from the remaining 18 ns of MD trajectories for the free energy calculations. Water molecules were stripped from these snapshots for binding energy calculations. The contributions to the total free energy of binding include Coulombic interactions ($E_{electrostatic}$),

electrostatic energy was decomposed based on charge distribution within the GB model [59]. The decomposition of desolvation free energies, ΔG_{GB} and $\Delta G_{nonpolar}$, was applied based on linear combination of pairwise overlaps (LCPO) method. When decomposing the binding free energy contributions into amino acid residues, the method of Fisher et al. [62] was used to calculate the translational, rotational, and vibrational entropies.

3.3 RESULTS AND DISCUSSION

3.3.1 TRPC6 PEPTIDE DOCKING.

An initial study was performed to validate the docking protocol, as well as the computational definition of the FKBP12 receptor and the peptides as ligands. Docking of the $^{193}\text{LPLLVQRTIAR}^{203}$ peptide from TGF β TRI was performed with the computational model of the FKBP12 receptor in order to validate the docking procedure. This computational method did indeed reproduce the experimentally-derived binding mode of the TGF β TRI peptide with FKBP12, with a root-mean square deviation (RMSD) of 1.7 Å, as displayed in Figure 3.2.

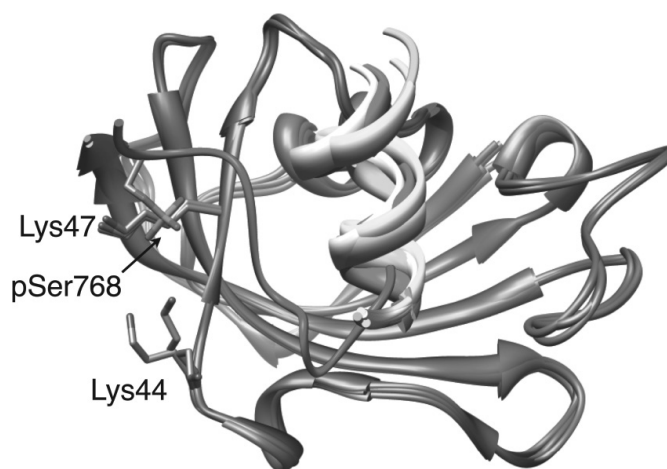


FIGURE 3.2 Superimposed crystal structures of FKBP12 with TFG β receptor peptide (PDB code: 1BC6, LPLLVQRTIAR), bone morphogenetic protein receptor type-1B peptide (PDB code: 3MDY, LPLLVQRTIAK) and kinase domain of the type I activin receptor peptide (PDB code: 3H9R, LPFLVQRTVAR). RMSD value between docked and crystal TFG β receptor peptide is 1.72 Å.

Given this increased confidence in our computational procedure and the experimental precedent for FKBP12 binding to α -helical domains (PDB code: 1B6C, 3H9R and 3MDY), docking of four TRPC6 peptides to FKBP12 was subsequently performed. The unphosphorylated (WT) and phosphoSer768 wild-type (pWT) TRPC6 peptides, as well as Ser768Asp and Ser768Glu mutants of TRPC6 were oriented into the FKBP12 binding pocket. From this point forward, the unphosphorylated and phosphorylated wild-type peptide will be referred as WT and pWT, respectively. The two mutants will be referred to as Ser768Asp and Ser768Glu, respectively. The top-scoring binding modes for the TGF β TRI and pWT peptides are displayed in Figure 3.2. On the basis of the DOCK energy score, the most energetically-favorable binding modes of the TRPC6 peptides reveal a different orientation relative to the experimental binding mode of the TGF β TRI peptide. The energy scores for peptides containing a negatively-charged amino acid at position 768 are dominated by a significant electrostatic contribution (Table 3.1), resulting from the binding of the anionic side chain between two surface lysine residues of FKBP12 (Lys44 and Lys47). These lysine residues do not establish interactions with the α -helical binding domain of TGF β TRI, bone morphogenetic protein receptor type-1B, or the kinase domain of the type I activin receptor (Figure 3.2). Furthermore, crystal structures indicate these residues do not contact FK506 [63].

Direct structural characterization of the delicate interactions constituting the phosphorylated TRPC6-FKBP12 binding interface pose difficulties for experiment. Thus, we employed MD simulations in explicit solvent to characterize the features of FKBP12 important for recognition of this phosphoprotein. These MD simulations were used to evaluate the stability of the protein-peptide complexes and to highlight the important residues involved in mediating these interactions. In combination with equivalent simulations of the isolated species, these simulations allowed the computation of the binding free energies of the various peptides to FKBP12.

3.3.2 RMSD OF FKBP12-PEPTIDE COMPLEXES

We computed the RMSD deviation for the FKBP12-peptide complexes over the course of each 20 ns MD simulation relative to the initial coordinates

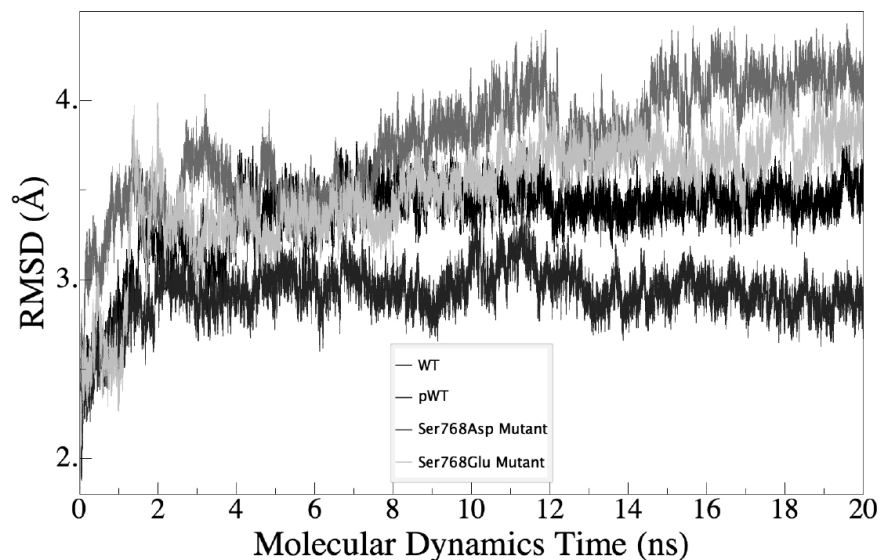


FIGURE 3.3 RMSD of the four complexes during 20 ns MD simulations.

of the production MD simulation (Figure 3.3). All of the protein atoms were included in the RMSD calculations. During the first 2 ns, the RMSD values increased to ~ 3 Å. Beyond this time, each protein-peptide complex remained stable for the course of the simulation, although there were notable differences in their relative flexibility as determined by decomposition of the RMSD values into each residue (*vide infra*). The average RMSD of the FKBP12-WT complex is 3.4 ± 0.1 Å. The complex containing the pWT peptide was more stable, with an average RMSD of 3.0 ± 0.1 Å from 3 to 20 ns. Apparently, phosphorylation of Ser768 restricts the conformational freedom of the protein-peptide complex, which could facilitate the formation of the multi-protein complex observed experimentally [12]. Due to the apparent importance of a negatively charged residue at position 768 of TRPC6, mutations were introduced in this position to test the hypothesis that that anionic amino acids would behave similarly to the phosphorylated peptide. The Ser768Asp and Ser768Glu peptides displayed greater RMSD (3.8 ± 0.3 Å and 3.6 ± 0.2 Å between 3 and 20 ns, respectively) in their respective MD trajectories than the WT peptides, despite their electrostatic similarity to the phosphorylated peptide. These simulations indicated that intrinsic properties of the phosphate functionality (or interactions other than electrostatic contributions of the negatively charged side chain) may contribute to TRPC6 binding.

To quantify changes in individual FKBP12 residues as a result of peptide binding, the RMSD of each residue relative to those of an isolated FKBP12 trajectory were calculated (Figure 3.3). WT- and pWT-bound FKBP12 residues demonstrate comparable values to unbound FKBP12. In contrast, regions of the Ser768Asp- and Ser768Glu-FKBP12 complexes displayed larger RMSD values than unbound FKBP12, especially in the ⁹PGDGRTFPKRG¹⁹ (referred as 10 loop), ³¹EDGKKF³⁶ (30 loop) and ⁸⁴ATGHPGIIPPH⁹⁴ (80–90) regions (Figure 3.4).

Gohlke and Case [64] proposed two approaches for computing binding free energies using the MM-GB/SA method. The single-trajectory approach relies upon the MD trajectories of the protein-protein complex alone, hence all of the necessary trajectory frames of each binding partner are extracted from the complex trajectories. The alternative separate-trajectory approach requires independent MD simulations of the protein-protein complex and the isolated binding partners. The computational economy of the single-trajectory approach is obvious. However, a limitation of the single-trajectory approach is that its accuracy depends on whether the binding partners undergo significant conformational changes during the binding event. When different results arise from these two approaches, the separate-trajectory approach is considered to be more reliable, since each entity is independently simulated to model its actual state before and after binding. Although both approaches were applied in the present study, the remainder

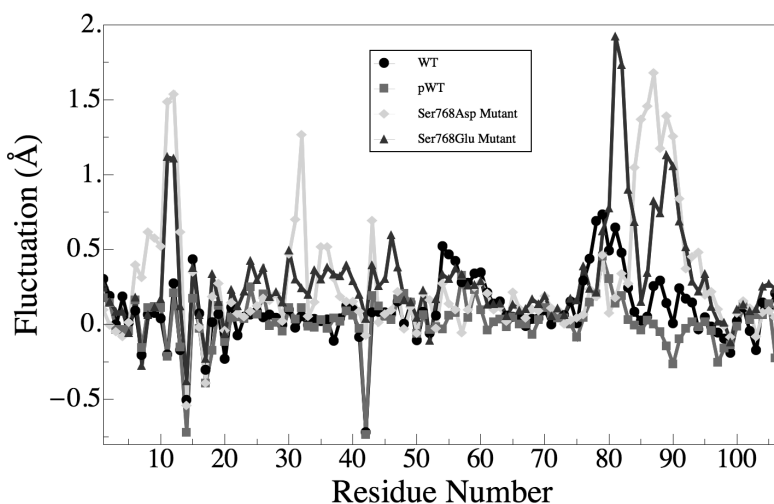


FIGURE 3.4 Average residue fluctuation of FKBP12 in MD simulations relative to isolated FKBP12.

of the discussion is primarily devoted to the results obtained considering separate trajectories of the binding partners. Unless otherwise noted, single-trajectory results are reserved for the Supporting Information.

3.3.3 FREE ENERGY OF BINDING CALCULATIONS

Calculated binding free energies of the four complexes using their respective MD trajectories are listed in Table 3.3. All of the energy terms and their corresponding standard errors calculated by the MM-GB/SA method are provided in the Supporting Information (Table 3.4). Using the separate-trajectory approach, the free energy of the pWT-FKBP12 complex was calculated to be 4.8 kcal/mol, only 0.9 kcal/mol different from result based on single-trajectory method (Table 3.3). This result indicates that the FKBP12 and pWT binding event does not involve significant overall conformational changes.

In contrast, the difference in the free energies of binding calculated by the two methods for the FKBP12-WT complex is much larger (~10 kcal/mol). The result based on separate-trajectory method is consistent with the experimental observation that FKBP12 does not bind unphosphorylated TRPC6 *in vitro* [12]. Accurate calculation of binding free energies using the single-trajectory approach requires that the isolated binding partners maintain their unbound conformations in the complex; hence it possible that phosphorylation conformationally restrains the peptide for binding to FKBP12. The free energy required to induce this conformational shift of the unphosphorylated peptide in the single-trajectory approach is absent, resulting in an erroneous prediction of the binding energy.

TABLE 3.3 Binding Free Energy (kcal/mol) of FKBP12 and Peptide Complexes^a

TRPC6 peptide	Single-trajectory	Separate-trajectory
WT	-5.4	4.5
pWT	-5.7	-4.8
Ser768Asp	1.3	28.0
Ser768Glu	0.0	14.1

^aEntropic contribution to the binding free energy was calculated using normal mode analysis (NMODE in AMBER).

TABLE 3.4 Binding Free Energy Components of FKBP12 and Probe Peptides Complexes

FKBP12 and Wild type TRPC6 Peptide Complex												
Contributions (kcal/mol) ^a	FKBP12- Wild-type Complex	FKBP12 (bound)	Average σ^b	Wild-type (bound)	Average σ^b	Delta Average ^c	FKBP12 (unbound)	Wild-type (unbound)	Delta Average ^d			
$E_{\text{electrostatic}}$	-2651.3	59.6	-2502.3	60.7	-107.1	6.8	-42.0	-2521.7	63.6	-105.4	8.8	-24.2
E_{vdw}	-474.5	18.4	-409.0	18.0	-8.9	4.7	-56.6	-418.1	15.5	-8.5	6.1	-47.9
E_{internal}	2515.4	29.7	2242.1	27.9	273.3	10.0	0.0	2244.1	27.8	267.7	9.7	3.6
E_{gas}	-610.5	65.6	-669.2	66.1	157.3	11.3	-98.6	-695.7	66.7	153.8	13.5	-68.5
G_{nonpolar}	48.5	1.0	46.9	1.0	10.1	0.2	-8.5	46.9	0.8	10.3	0.5	-8.7
G_{GB}	-1328.4	56.6	-1321.8	57.2	-76.1	5.0	69.5	-1302.3	57.1	-75.7	7.3	49.7
$G_{\text{solvation}}$	-1279.9	56.0	-1274.9	56.7	-66.0	5.0	61.1	-1255.5	56.7	-65.4	7.0	41.1
$E_{\text{gas}} + G_{\text{solvation}}$	-1890.3	29.7	-1944.1	28.5	91.3	10.0	-37.5	-1951.2	28.3	88.3	10.1	-27.5
TS_{total}	1348.9	10.6	1230.1	10.1	150.9	3.1	-32.1	1228.8	10.2	152.0	3.7	-31.9
$\Delta G_{\text{binding}}$							-5.4					4.5

FKBP12 and Phosphorylated Wild type TRPC6 Peptide Complex												
Contributions (kcal/mol) ^a	FKBP12- Phosphorylated Wild-type	FKBP12 (bound)	Average σ^b	Phosphorylated Wild-type (bound)	Average σ^b	Delta Average ^c	FKBP12 (unbound)	Phosphorylated Wild-type (unbound)	Delta Average ^d			
$E_{\text{electrostatic}}$	-2901.6	73.3	-2508.1	61.1	-160.9	38.0	-232.6	-2521.7	63.6	-184.8	22.1	-195.1
E_{vdw}	-466.4	17.2	-410.3	16.1	-6.6	4.8	-49.4	-418.1	15.5	-6.1	5.3	-42.2
E_{internal}	2528.4	29.9	2242.2	28.2	286.2	10.6	0.0	2244.1	27.8	282.7	9.7	1.7

TABLE 3.4 (Continued)

E_{gas}	-839.5	73.5	-676.2	64.0	118.7	34.7	-282.0	-695.7	66.7	91.8	22.2	-235.6		
G_{GB}	-1375.8	65.0	-1321.7	55.3	-301.3	36.0	247.2	-1302.3	57.1	-277.1	20.4	203.7		
$G_{\text{solvation}}$	-1326.6	64.7	-1275.0	55.0	-290.6	35.6	239.0	-1255.5	56.7	-266.3	20.3	195.2		
$E_{\text{gas}} + G_{\text{solvation}}$	-2166.2	29.7	-1951.2	28.1	-171.9	10.1	-43.1	-1951.2	28.3	-174.5	9.5	-40.4		
TS	1350.7	9.9	1229.7	10.0	158.5	4.7	-37.4	1228.8	10.2	157.8	4.0	-35.6		
$\Delta G_{\text{binding}}$							-5.7					-4.8		
FKBP12 and TRPC6 Peptide with Mutation Ser768Asp Complex														
Contributions (kcal/mol) ^a	FKBP12- Mutant (Ser768Asp)		FKBP12 (bound)		Mutant (Ser768Asp) (bound)		Delta Average ^c		FKBP12 (unbound)		Mutant (Ser768Asp) (unbound)		Delta Average ^d	
	Average	σ^b	Average	σ^b	Average	σ^b	Average	σ^b	Average	σ^b	Average	σ^b	Average	σ^b
$E_{\text{electrostatic}}$	-2681.0	82.0	-2461.0	91.2	-81.1	6.7	-138.9	-2521.7	63.6	-79.9	8.6	-79.4		
E_{vdw}	-461.5	19.8	-406.2	17.4	-10.7	4.7	-44.5	-418.1	15.5	-8.5	6.1	-35.0		
E_{internal}	2520.3	29.2	2244.7	27.9	275.6	9.0	-0.0	2244.1	27.8	266.6	8.9	9.7		
E_{gas}	-622.1	84.9	-622.5	91.9	183.8	10.8	-183.4	-695.7	66.7	178.3	13.6	-104.7		
G_{nonpolar}	49.9	1.1	47.7	1.0	9.8	0.2	-7.6	46.9	0.8	10.8	0.7	-7.8		
G_{GB}	-1349.1	70.5	-1354.2	79.2	-153.4	6.1	158.5	-1302.3	57.1	-150.5	7.3	103.8		
$G_{\text{solvation}}$	-1299.1	70.2	-1306.4	79.0	-143.6	6.0	150.9	-1255.5	56.7	-139.7	7.0	96.1		
$E_{\text{gas}} + G_{\text{solvation}}$	-1921.3	31.9	-1928.9	29.8	40.1	9.0	-32.5	-1951.2	28.3	38.6	10.1	-8.6		
TS	1349.1	10.8	1231.4	9.8	151.6	2.6	-33.9	1228.8	10.2	156.9	4.1	-36.7		
$\Delta G_{\text{binding}}$							1.3					28.0		

TABLE 3.4 (Continued)

FKBP12 and TRPC6 Peptide with Mutation Ser768Glu Complex												
Contributions (kcal/mol) ^a	FKBP12-Mutant (Ser768Glu)	FKBP12 (bound)	Mutant (Ser768Glu) (bound)	Delta Average ^c	FKBP12 (unbound)	Mutant (Ser768Glu) (unbound)	Delta Average ^c	Mutant (Ser768Glu) (unbound)	Delta Average ^d			
	Average σ^b	Average σ^b	Average σ^b	Average σ^b	Average σ^b	Average σ^b	Average σ^b	Average σ^b	Average σ^b			
$E_{\text{electrostatic}}$	-2661.6	70.5	-2474.5	67.8	-105.0	8.7	-82.1	-2521.7	63.6	-94.8	9.7	-45.1
E_{vdw}	-459.1	16.7	-395.1	15.5	-11.9	4.5	-52.2	-418.1	15.5	-8.0	5.4	-33.0
E_{internal}	2515.0	29.3	2239.8	27.6	275.2	9.5	-0.0	2244.1	27.8	271.1	9.5	-0.1
E_{gas}	-605.7	76.6	-629.7	73.8	158.3	12.8	-134.3	-695.7	66.7	168.3	12.7	-78.3
G_{nonpolar}	50.2	1.0	48.8	0.9	2.6	9.4	-8.9	46.9	0.8	10.8	0.5	-7.5
G_{GB}	-1406.2	66.6	-1350.0	63.9	10.3	0.2	105.4	-1302.3	57.1	-168.2	8.3	64.4
$G_{\text{solvation}}$	-1356.0	66.0	-1301.2	63.3	-161.6	8.3	96.5	-1255.5	56.7	-157.4	8.2	56.9
$E_{\text{gas}} + G_{\text{solvation}}$	-1961.7	30.7	-1931.0	29.4	7.1	9.4	-37.8	-1951.2	28.3	10.9	10.1	-21.3
TS	1352.0	10.7	1234.4	10.6	155.3	2.9	-37.7	1228.8	10.2	158.7	4.0	-35.5
$\Delta G_{\text{binding}}$							-0.0					14.1

^a $E_{\text{electrostatic}}$: Coulombic energy; E_{vdw} : van der Waals energy; E_{internal} : internal energy; E_{gas} : gas electrostatic energy; $E_{\text{vdw}} + E_{\text{internal}}$: nonpolar solvation free energy; G_{GB} : polar solvation free energy; $G_{\text{solvation}} = G_{\text{nonpolar}} + G_{\text{GB}}$: total entropy contribution by normal mode analysis; $\Delta G_{\text{binding}} = E_{\text{gas}} + G_{\text{solvation}} - TS_{\text{total}}$

^bStandard error of average values.

^cCalculation based on trajectory of complex only.

^dCalculation based on separated trajectories of complex, FKBP12 and TRPC6 peptides.

Surprisingly, the mutants Ser768Asp and Ser768Glu are not predicted to have thermodynamically-favorable binding energies with FKBP12. This observation suggests these mutants cannot constitutively mimic the phosphoserine necessary for FKBP12 binding.

3.3.4 SEPARATE-TRAJECTORY FREE ENERGY OF BINDING DECOMPOSITION ANALYSIS

The free energies of binding based on the separate-trajectory approach were decomposed into each residue with the entropic contribution computed with the method of Fisher et al. (Figures 3.5–3.7) In the pWT complex, several peptide residues (Leu759, Pro760, Val761, and Asn764) contribute significantly to the binding free energies. Notably, the N-terminal LP residues are conserved in of the FKBP12 recognition sequences. pSer768 also contributes a positive contribution to the binding free energy, although it is approximately one-third (+2.1 kcal/mol) of that

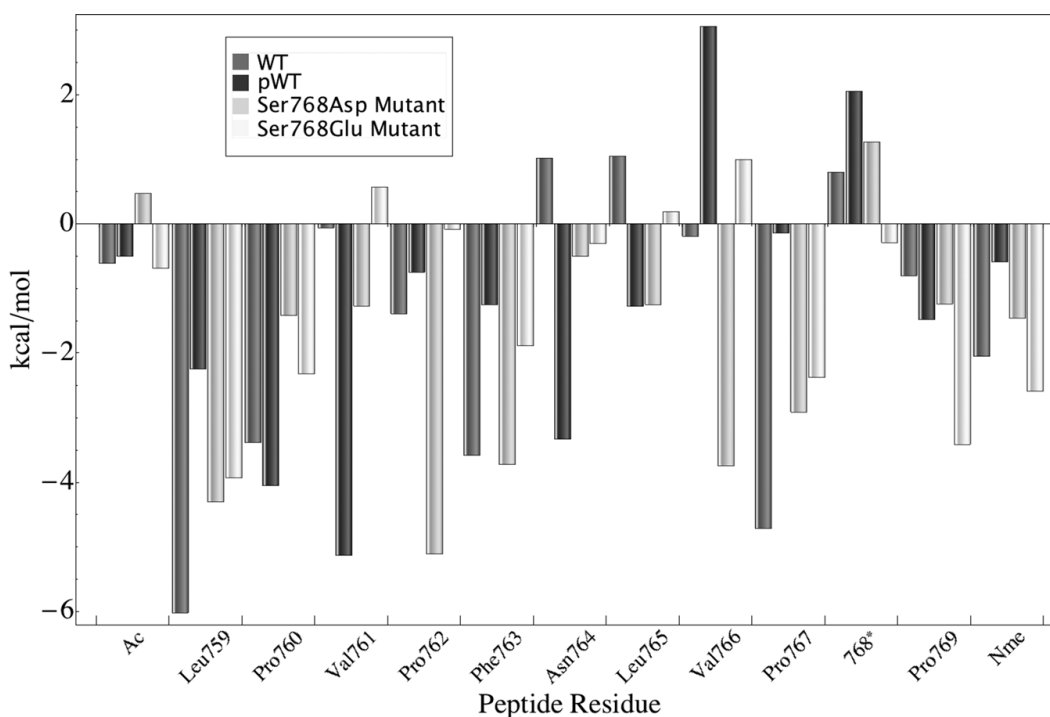


FIGURE 3.5 Decomposition of binding free energies into single residues of peptide based on separated MD trajectories.

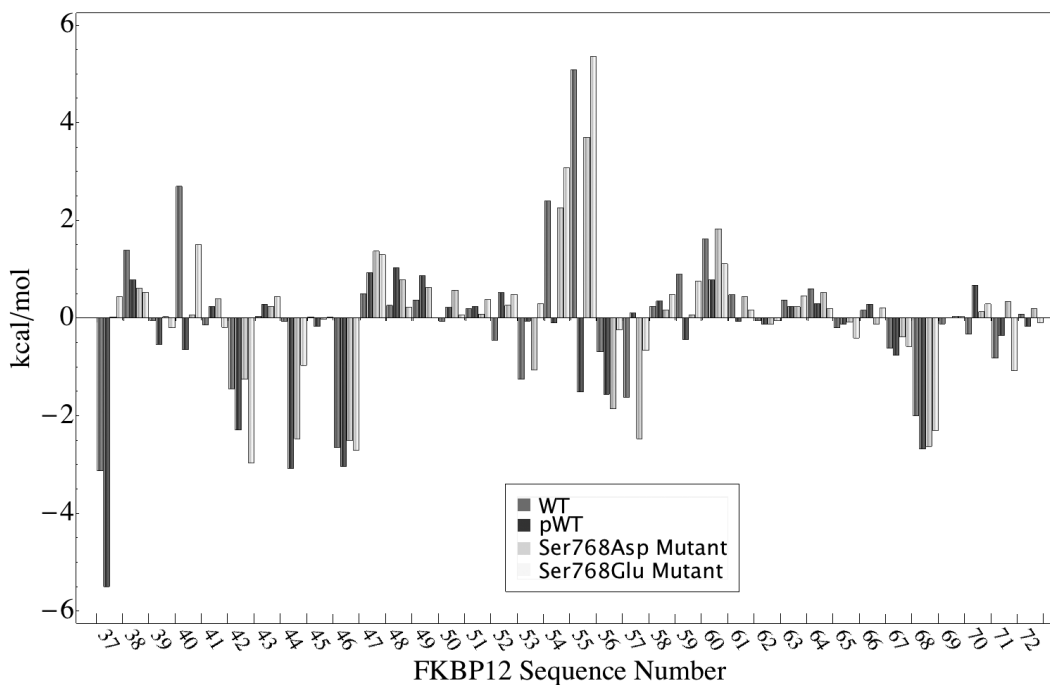


FIGURE 3.6 Decomposition of binding free energies into single residues of FKBP12 (residues 37 to 72) based on separated MD trajectories.

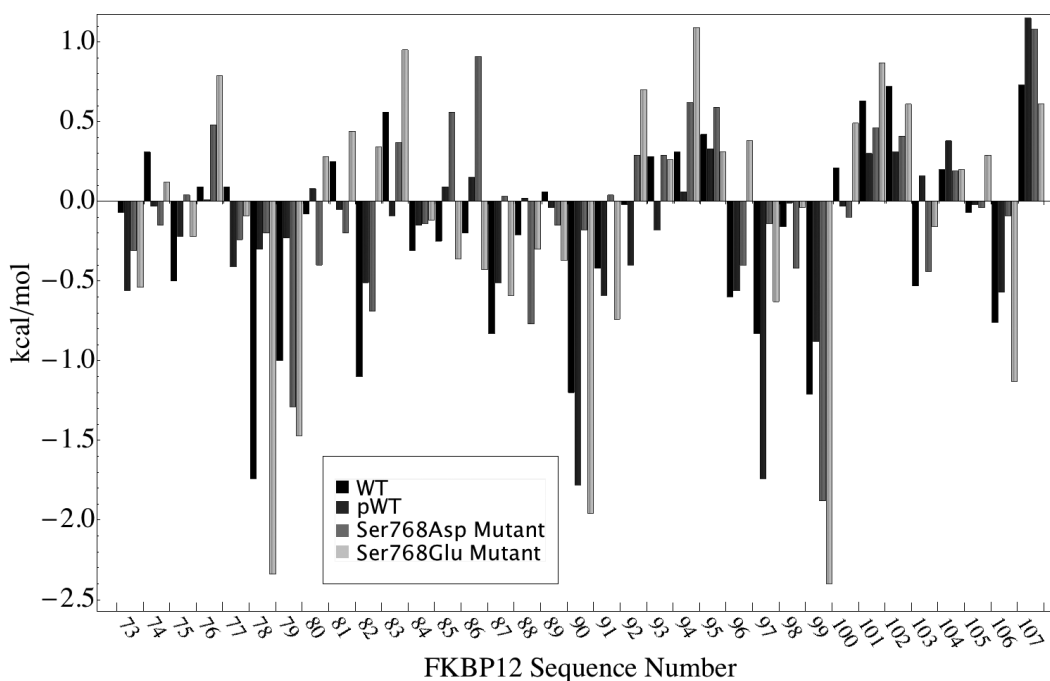


FIGURE 3.7 Decomposition of the binding free energies (from separate trajectory approach) into FKBP12 residues 73–107.

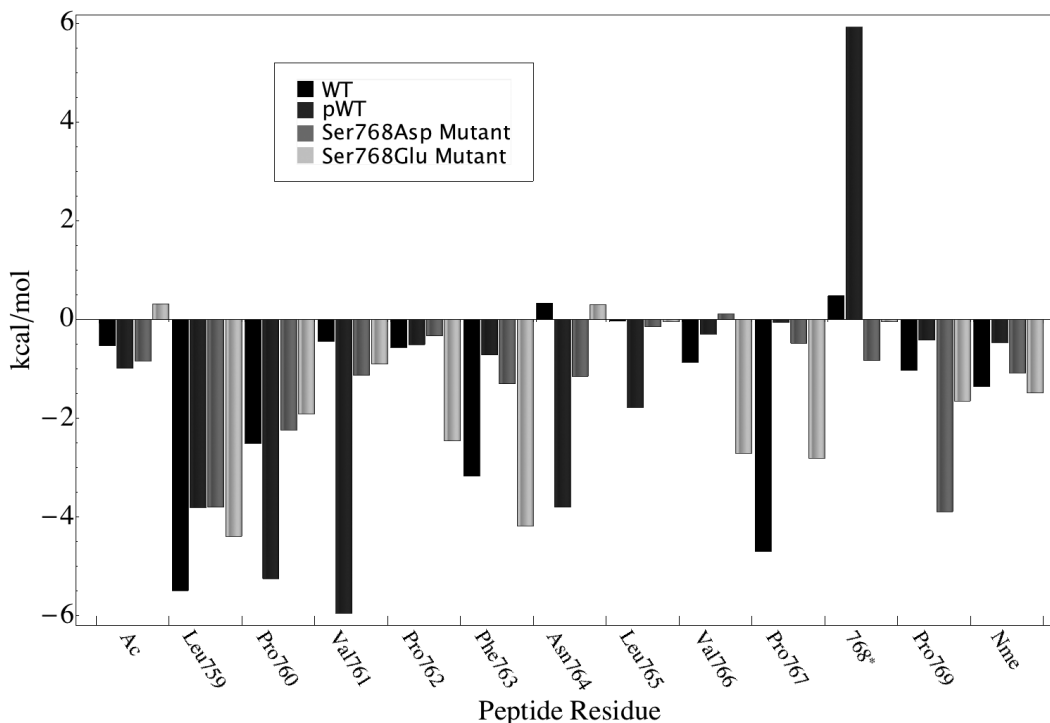


FIGURE 3.8 Decomposition of the binding free energies into single residues in the TRPC6 peptides. Data are based on single MD trajectory.

calculated in the single-trajectory approach (Figure 3.8). The unfavorable contribution (+0.9 kcal/mol) of FKBP12 Lys47 (Figure 3.6) was surprising, and may be due to the limited frames used for the binding free energy calculation (*vide infra*). Nevertheless, the negative contribution of FKBP12 Lys44 (−3.1 kcal/mol) offsets the small positive contributions of peptide pSer768 and FKBP12 Lys47. The results of the energetic decomposition analysis are rather different for the other three complexes. It is interesting to note that the decomposed contributions of some residues from WT and Ser768Asp peptides to binding free energies are somewhat more favorable in separate-trajectory results than in single-trajectory results (Figures 3.5 and 3.8). However, contributions from FKBP12 to binding free energies in these two complexes are more unfavorable in separate-trajectory results than in single-trajectory results.

In the pWT complex, both hydrophobic and hydrophilic residues from FKBP12 make significant contributions to binding affinity. Hydrophobic residues are evenly arranged at the bottom of the FKBP12 binding site (Figure 3.9), forming a hydrophobic pocket to host the peptide ligand.

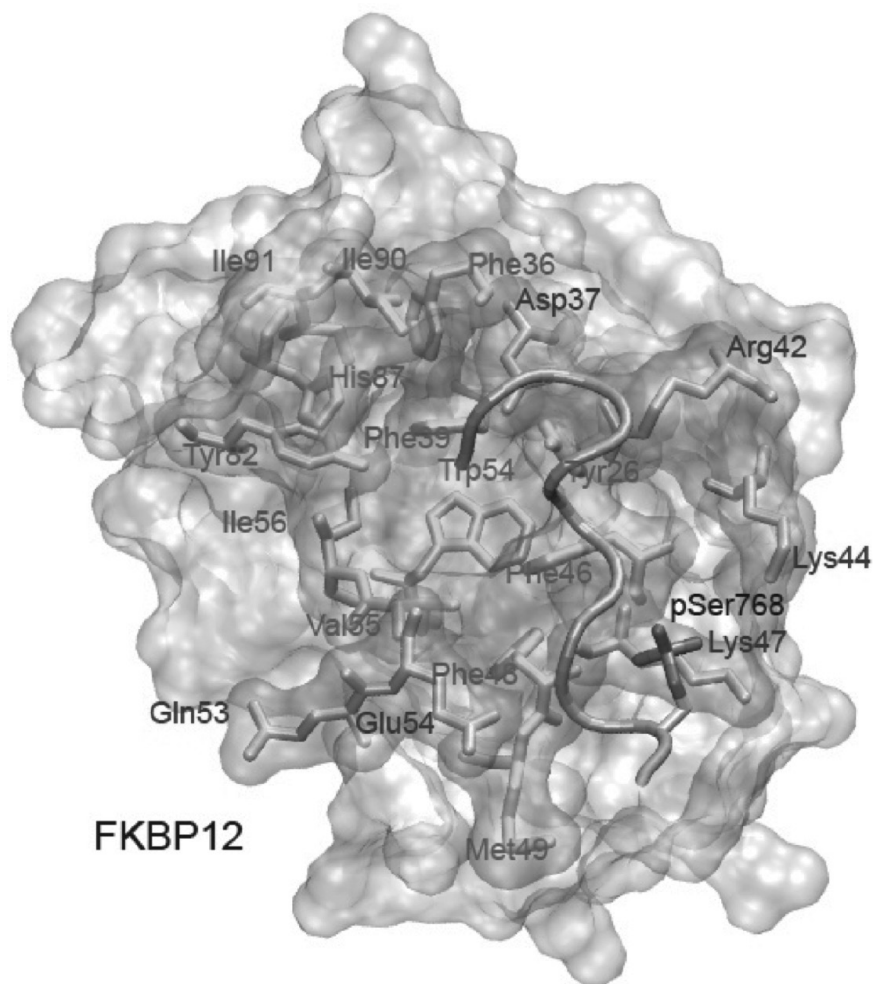


FIGURE 3.9 Residues with significant contribution to the total binding free energy at the binding site of FKBP12. Hydrophobic residues: Tyr26, Phe36, Phe39, Phe46, Phe48, Met49, Trp54, Val55, Ile56, Tyr2, His87, Ile90, and Ile91. Hydrophilic residues: Asp37, Arg42, Lys44, Lys47, Glu54, and Gln53.

Phe36, Val55, Ile56, Trp59, and Phe99 are located at the bottom of the binding pocket. His87, Ile90, and Ile91 (from the 80–90 loop) form a hydrophobic wall on one side, while Phe46, Phe48 and Met49 form another hydrophobic wall on the opposite side. Overall, these residues form a large, “U-shaped” hydrophobic pocket to host the N-terminal end of the peptide. A number of hydrophilic residues with hydrogen-bonding and ion pair interaction capabilities are arranged above the rim of this hydrophobic cavity (Figure 3.9). Asp37, Arg42, Lys44 and Lys47 are located on one side, while Gln53 and Glu54 are on the other side of the hydrophobic cavity.

3.3.5 INTERACTIONS AMONG FKBP12 LYS44, LYS47 AND PEPTIDE RESIDUE 768

Despite the apparently unfavorable energetic contribution of Lys47 predicted by decomposition of the separate-trajectory data, single-trajectory data and pairwise distance analyzes support both Lys residues being important for interaction with pSer768 (Figure 3.10). In the FKBP12-WT complex (Figure 3.10A), Ser768 does not have a stable interaction either Lys residues. By contrast, the pSer768 maintains stable interactions with the Lys residues throughout the MD simulation (Figure 3.10B). In the early stages of the MD simulation, the peptide phosphoserine residue is strongly coupled to FKBP12 Lys47. The pSer768-O γ to Lys47-N ϵ distance remains ~ 5 Å, while the pSer768-O γ to Lys44-N ϵ and Lys44-N ϵ to Lys47-N ϵ distances are much longer (>10 Å). The two FKBP12 lysines residues approach one another and at 7.1 ns achieve a minimum distance of 3.8 Å. The negative charge of the phosphate group apparently screens

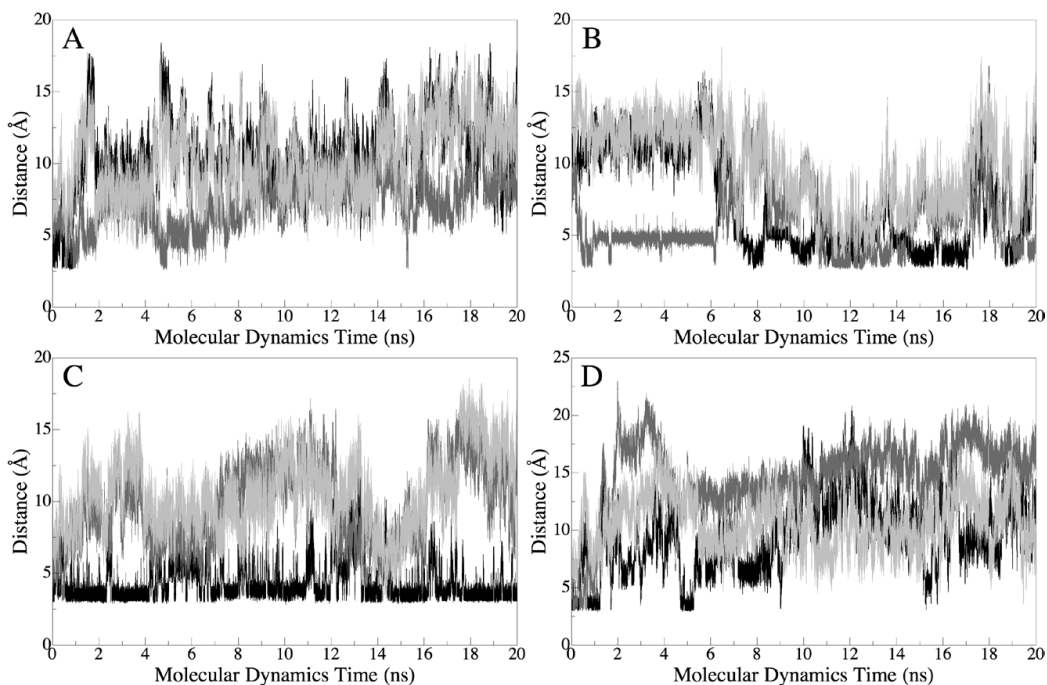


FIGURE 3.10 Atomic pair distance analysis for Lys44, Lys47 and Residue 768 from probe peptides. A. WT complex (Lys44-N ϵ :Ser768-O γ , black; Lys47-N ϵ :Ser768-O γ , dark gray; Lys44-N ϵ :Lys47-N ϵ , light gray); B. pWT complex (Lys44-N ϵ :pSer768-O γ , black; Lys47-N ϵ :pSer768-O γ , dark gray; Lys44-N ϵ :Lys47-N ϵ , light gray); C. Ser768Asp complex, (Lys44-N ϵ :Asp768-C γ , black; Lys47-N ϵ : Asp768-C γ , dark gray; Lys44-N ϵ :Lys47-N ϵ , light gray); D. Ser768Glu complex, (Lys44-N ϵ :Glu768-C δ , black; Lys47-N ϵ :Glu768-C δ , dark gray; Lys44-N ϵ :Lys47-N ϵ , light gray).

the repulsion between the lysines, allowing them to approach each other and transfer the salt bridge. The close approach of the two lysine amino groups allow transfer of the ion pair interaction with the peptide phosphoserine to FKBP12 Lys44. This switching occurs four times throughout the 20 ns MD simulation. This process is illustrated in Figure 3.11. After each switch, either FKBP12 Lys44 or Lys47 remains in close contact with the peptide phosphoserine residue, indicating that the two lysine residues are equally important when interacting with the phosphate group.

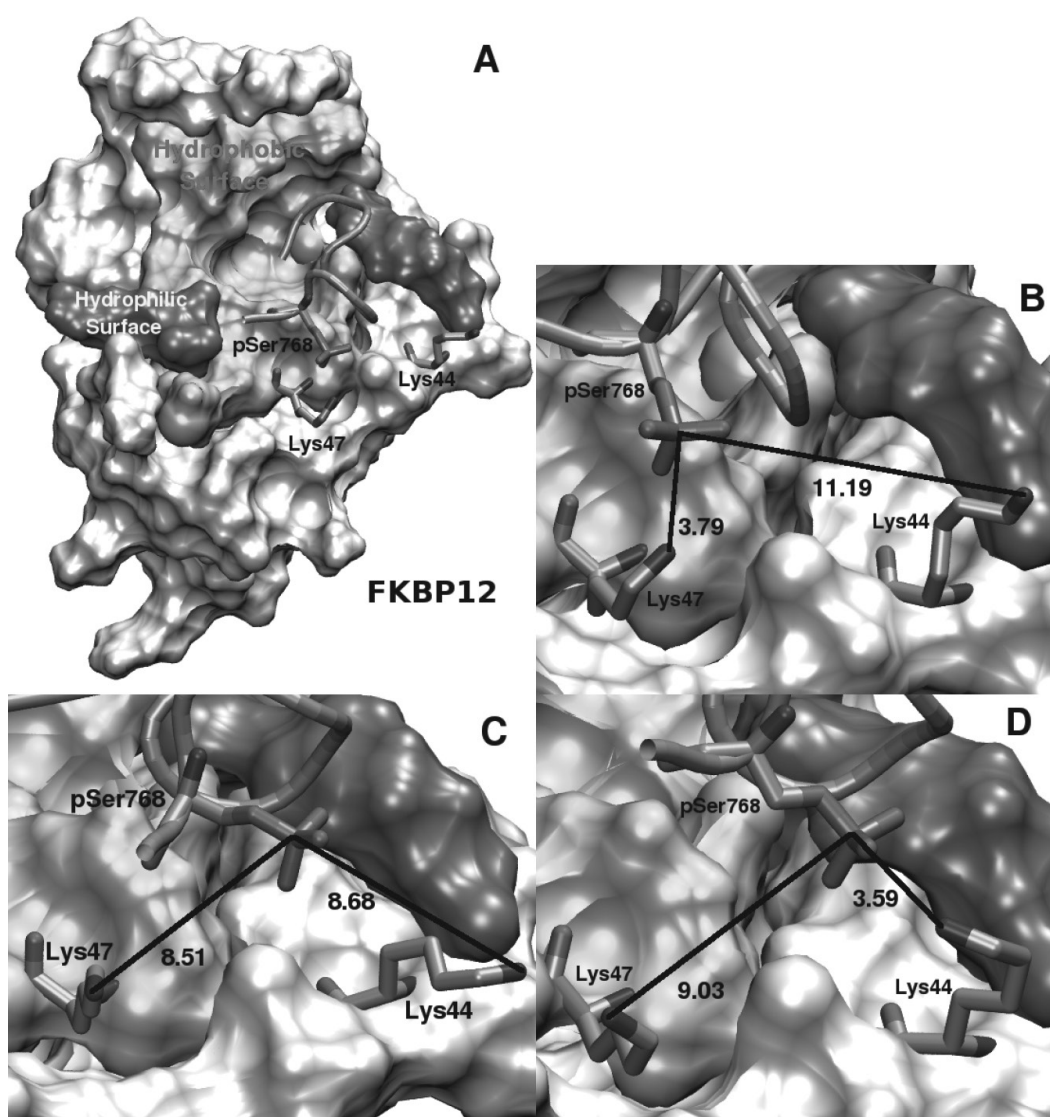


FIGURE 3.11 Transient ionic interaction between the pWT phosphoSer768 and FKBP12 Lysines 44 and 47: (a) surface of FKBP12, (b) phosphate group forming salt bridge with Lys47, (c) transition state during switch, (d) phosphate group forming salt bridge with Lys44. Distances are in Å.

In the Ser768Asp mutant complex, the peptide Asp768 residue has a close contact with the Lys44 of FKBP12. This observation supports our hypothesis that the carboxylate side chain is capable of mimicking the anionic character of the phosphoserine by forming an apparent ion pair. However, the carboxylate side chain cannot recruit both lysines for interaction when bound to FKBP12. (Figure 3.10C) After 5 ns of the MD simulation involving the Ser768Asp peptide, the FKBP12 Lys47 amino group approaches γ -carbon of peptide Asp768 (Asp768-C γ), with a concomitant increase in the Lys44-N ϵ -Asp768-C γ distance. Between 5 to 7 ns, these side chains remain within 5 to 8 Å. Despite the approach of FKBP12 Lys47 several times during the simulation, the apparent salt bridge involving the carboxylate unit is not transferred to Lys44. Beyond 7 ns, FKBP12 Lys47 returns to the previous configuration. An analogous trajectory consistent with another ‘switch’ of the cationic partner occurs between 14 and 15 ns, but is also unsuccessful. Indeed, the anionic side chain in the Ser768Asp peptide forms an apparent salt bridge with one of the Lys residues, however; the carboxylate unit is not sufficient to recruit both FKBP12 Lys44 and 47 as cationic partners, as is observed in the pWT peptide. The dual recruitment of these lysine residues appears to be a prerequisite for favorable binding affinity.

The Ser768Glu mutant (Figure 3.10D) behaves quite differently from the Ser768Asp mutant. First, peptide Glu768 cannot maintain close contact with FKBP12 Lys44. Although the Lys44-N ϵ and δ carbon of peptide Glu768 (Glu768C δ) can approach one another within 3 Å to form salt bridge briefly at 5 ns of simulation, the dynamics of FKBP12 Lys44 and peptide Glu768 are not strongly coupled through the course of our simulation. Instead, this distance fluctuates between 5 to 15 Å afterward. The distance from Glu768-C δ to Lys47-N ϵ is much longer than to Lys44-N ϵ . Peptide Glu768 appears to be ineffective in involving interaction with both lysine residues. From comparing the behavior of the two Ser768 mutants, we see that while glutamate and aspartate residues differ by only one side-chain methylene unit, this small structural difference causes large deviations in protein-protein interactions.

3.4 CONCLUSIONS

In this study, we have applied MD simulations to study interactions between FKBP12 and TRPC6 channel peptides. Experiments suggest phosphorylation of Ser768 in the TRPC6 intracellular domain is a prerequisite for

FKBP12 binding and subsequent formation of a multiprotein complex. The FKBP12-pWT complex is the most stable and the least flexible among the studied peptide complexes. Both Ser768Asp and Ser768Glu complexes have larger RMSD than those in the pWT complex. The calculated free energies of binding showed that the pWT peptide but not WT peptide has a thermodynamically favorable binding affinity with FKBP12, consistent with experimental data. Neither the Ser768Asp nor Ser768Glu mutants demonstrate a thermodynamically favorable binding affinity with FKBP12. These calculations indicate these mutants cannot constitutively mimic the phosphoserine residue, which is necessary for FKBP12 binding.

The decomposition of binding free energies into individual residues of the FKBP12 and TRPC6 peptide revealed a specific binding pocket composed of both hydrophobic and hydrophilic residues for the recognition and interaction of FKBP12 with the TRPC6 intracellular domain. About twenty residues, including both hydrophobic and hydrophilic residues contributed significantly to the FKBP12-TRPC6 binding energy. Hydrophobic residues formed a “U” shaped binding pocket to recognize hydrophobic residues in the TRPC6 binding domain. Lys44 and Lys47, surrounding the rim of the hydrophobic cavity, apparently contribute the key elements for recognition of the phosphopeptide.

ACKNOWLEDGMENTS

The authors are indebted to the Ohio Supercomputer Center for computational resources.

KEYWORDS

- **FKBP12**
- **free energy**
- **MM-GB/SA**
- **molecular dynamics**
- **molecular recognition**
- **TRPC6**

REFERENCES

1. Ramsey, I. S., Delling, M; & Clapham, D. E. (2006). *Annu. Rev. Physiol.* 68, 619.
2. Wu, L.J; Sweet T. B., & Clapham, D. E. (2010). *Pharmacol. Rev.* 62, 381,
3. Li, S., Westwick, J., & Poll, C. T. (2002). *Trends Pharmacol. Sci.* 23, 63.
4. Ong, H. L., & Barritt, G. J. (2004). *Respirology* 9, 448.
5. Harteneck C., & Gollasch, M. (2011). *Curr. Pharm. Biotechnol.* 12, 35
6. Morelli M. B., Amantini, C., Liberati, S; Santoni, M., & Nabissi, M. (2013). *CNS Neurol. Disord. Drug Targets* 12, 274
7. Trebak, M., Vazquez, G., Bird, G. S., & Putney, J. W. Jr. (2003). *Cell Calcium* 33, 451.
8. Dietrich, A., Kalwa, H., Rost, B. R., & Gudermann, T. (2005). *Pflugers Arch.* 451, 72.
9. Yao, X., Kwan, H. Y., & Huang, Y. (2005). *Neurosignals*, 14, 273.
10. Kiselyov, K., Kim, J. Y., Zeng, W., & Muallem, S. (2005). *Pflugers Arch.* 451, 116.
11. Trebak, M., Hempel, N., Wedel, B. J., Smyth, J. T., Bird, G. S., & Putney, J. W. (2005). *Mol. Pharmacol.* 67, 558.
12. Kim, J. Y., & Saffen, D. (2005). *J. Biol. Chem.* 280, 32035.
13. Vazquez, G., Wedel, B. J., Kawasaki, B. T., Bird, G. S., & Putney, J. W. Jr., (2004). *J. Biol. Chem.* 279, 40521.
14. Hisatsune, C., Kuroda, Y., Nakamura, K., Inoue, T., Nakamura, T., Michikawa, T., Mizutani, A., & Mikoshiba, K. (2004). *J. Biol. Chem.* 279, 18887.
15. Zhang, Z., Tang, J., Tikunova, S., Johnson, J. D., Chen, Z., Qin, N., Dietrich, A., Stefani, E., Birnbaumer, L., & Zhu, M. X. (2001). *Proc. Natl. Acad. Sci. USA*, 98, 3168.
16. Tang, J., Lin, Y., Zhang, Z., Tikunova, S., Birnbaumer, L., & Zhu, M. X. (2001). *J. Biol. Chem.* 276, 21303.
17. Kiselyov, K., Xu, X., Mozhayeva, G., Kuo, T., Pessah, I., Mignery, G., Zhu, X., Birnbaumer, L., & Muallem, S. (1998). *Nature* 396, 478.
18. Yuan, J. P., Kiselyov, K., Shin, D. M., Chen, J., Shcheynikov, N., Kang, S. H., Dehoff, M. H., Schwarz, M. K., Seeburg, P. H., Muallem, S., & Worley, P. F. (2003). *Cell* 114, 777.
19. Kim, J. Y., Zeng, W., Kiselyov, K., Yuan, J. P., Dehoff, M. H., Mikoshiba, K., Worely, P. F., & Muallem, S. (2006). *J. Biol. Chem.* 281, 32540.
20. Sinkins, W. G., Goel, M., Estacion, M., & Schiling, W. P. (2004). *J. Biol. Chem.* 279, 34521.
21. Wang, W., Lim, W. A., Jakalian, A., Wang, J., Luo, R., Bayly, C. I., & Kollman, P. A., (2001). *J. Am. Chem. Soc.* 123, 3986.
22. Wang, J., Morin, P., Wang, W., & Kollman, P. A. (2001). *J. Am. Chem. Soc.* 123, 5221.
23. Swanson, J. M., Henchman, R. H., & McCammon, J. A. (2004). *Biophys. J.* 86, 67.
24. Srinivasan, J., Miller, J., Kollman, P. A., & Case D. A. *J. Biomol. Struct. Dyn.* (1998). 16, 671.
25. Reyes, C. M; & Kollman, P. A., *J. Mol. Biol.* (2000). 297, 1145.
26. Luo, C., Xu, L., Zheng, S., Luo, X., Shen, J., Jiang, H., Liu, X., & Zhou, M. (2005). *Proteins* 59, 742.
27. Huo, S., Massova, I., & Kollman, P. A. (2002). *J. Comput. Chem.* 23, 15.
28. Gouda, H., Kuntz, I. D., Case, D. A., & Kollman, P. A. (2003). *Biopolymers* 68, 16.
29. Fogolari, F., Brigo, A., & Molinari, H. (2003). *Biophys. J.* 85, 159.
30. Kollman, P. A., Massova, I., Reyes, C., Kuhn, B., Huo, S., Chong, L., Lee, M., Lee, T., Duan, Y., Wang, W., Donini, O., Cieplak, P., Srinivasan, J., Case, D. A., & Cheatham, T. E. III (2000). *Acc. Chem. Res.* 33, 889.

31. Onufriev, A., Bashford, D., & Case, D. A. (2004). *Proteins* 55, 383.
32. Fujitani, H; Tanida, Y; Ito, M; Jayachandran, G; Snow, C. D., Shirts, M. R., Sorin, E. J., & Pande, V. S. (2005). *J. Chem. Phys.* 123, 084108/1–084108/5.
33. Wang, J; Deng, Y; & Roux, B. (2006). *Biophys. J.* 91, 2798.
34. Deng, Y; & Roux, B. (2009). *J. Phys. Chem. B* 113, 2234.
35. Xu, Y., & Wang, R. (2006). *Proteins*, 64, 1058.
36. Lamb, M. L., Tirado-Rives, J., & Jorgensen, W. L. (1999). *Bioorg. Med. Chem.* 7, 851.
37. Huse, M., Chen, Y. G., Massague, J., & Kuriyan, J. (1999). *Cell* 96, 425.
38. Crystal structure of the cytoplasmic domain of the bone morphogenetic protein receptor type-1B (BMPRI1B) in complex with FKBP12 and LDN-19(3189). DOI:10.2210/pdb3mdy/pdb.
39. Crystal structure of the kinase domain of type I activin receptor (ACVR1) in complex with FKBP12 and dorsomorphin, DOI:10.2210/pdb3h9r/pdb.
40. Cornell, W. D., Cieplak, P., Bayly, C. I., Gould, I. R., Merz, K. M., Ferguson, D. M., Spellmeyer, D. C., Fox, T., Caldwell, J. W., & Kollman, P. A. (1995). *J. Am. Chem. Soc.* 117, 5179.
41. DOCK 5.20. Molecular Design Institute, University of California San Francisco. For more information see: <http://dock.compbio.ucsf.edu>.
42. Meng, E. C., Shoichet, B. K., & Kuntz, I. D. (1992). *J. Comput. Chem.* 13, 505.
43. Ewing, T. J. A., Makino, S., Skillman, A. G., & Kuntz, I. D. (2001). *J. Comput-Aided Mol. Design* 15, 411.
44. Case, D. A., Darden, T. A., Cheatham, III, T. E., Simmerling, C. L., Wang, J., Duke, R. E., Luo, R., Merz, K. M., Wang, B., Pearlman, D. A., Crowley, M., Brozell, S., Tsui, V., Gohlke, H., Mongan, J., Hornak, V., Cui, G., Beroza, P., Schafmeister, C., Caldwell, J. W., Ross, W. S., & Kollman, P. A. (2004). AMBER 8, University of California, San Francisco.
45. Duan, Y., Wu, C., Chowdhury, S., Lee, M. C., Xiong, G., Zhang, W., Yang, R., Cieplak, P., Luo, R., Lee, T., Caldwell, J., Wang, J., & Kollman, P. (2003). *J. Comput. Chem.* 24, 1999.
46. Jorgensen, W. L., Chandrasekhar, J., Madura J. D., Impey, R. W., & Klein, M. L. (1983). *J. Chem. Phys.* 79, 926.
47. Darden, T., York, D., & Pedersen, L. (1993). *J. Chem. Phys.* 98, 10089.
48. Essmann, U., Perera, L., Berkowitz, M. L., Darden, T., Lee H., & Pedersen, L. G. *J. Chem. Phys.* (1995). 103, 8577.
49. Crowley, M. F., Darden, T. A., Cheatham, T. E. III; & Deerfield, D. W. II. (1997). *J. Supercomput.* 11, 255.
50. Sagui, C., & Darden, T. A. (1999). *AIP Conf. Proc.*, 492, 104.
51. Toukmaji, A., Sagui, C., Board, J., & Darden, T. (2000). *J. Chem. Phys.* 113, 10913.
52. Ryckaert, J. -P., Ciccotti, G., & Berendsen, H. J. C. (1977). *J. Comput. Phys.* 23, 327.
53. Berendsen, H. J. C., Postma, J. P. M., Gunsteren, W. F. van; DiNola, A., & Haak, J. R. (1984). *J. Chem. Phys.* 81, 3684.
54. Srinivasan, J., Cheatham, III, T. E., Cieplak, P., Kollman P., & Case, D. A. (1998). *J. Am. Chem. Soc.* 120, 9401.
55. Wang, W., & Kollman, P. A. (2000). *J. Mol. Biol.* 303, 567.
56. Zhong, H., & Carlson, H. A. (2005). *Proteins* 58, 222.
57. Case, D. A. (1994). *Curr. Opin. Struct. Biol.* 4, 285.
58. Kottalam, J., & Case, D. A. (1990). *Biopolymers* 29, 1409.

59. Gohlke, H., Kiel, C., & Case, D. A. (2003). *J. Mol. Biol.* 330, 891.
60. Rarey, M., Kramer, B., Lengauer, T., & Klebe, G. (1996). *J. Mol. Biol.* 261, 470.
61. Weiser, J., Shenkin, P. S., & Still, W. C., (1999). *J. Comput. Chem.* 20, 217.
62. Fischer, S., Smith, J. C., & Verma, S. C. (2001). *J. Phys. Chem. B* 105, 8050.
63. Griffith, J. P., Kim, J. L., Kim, E. E., Sitchak, M. D., Thomson, J. A., Fitzgibbon, M. J., Fleming, M. A., Caron, P. R., Hsiao, K., & Navia, M. A. (1995). *Cell* 82, 507.
64. Gohlke, H., & Case, D. A. (2004). *J. Comput. Chem.* 25, 238.